Recognition of Cold-Water Corals in Synthetic Aperture Sonar Imagery

Øystein Sture, Martin Ludvigsen, Margrete S. Scheide
Department of Marine Technology
Norwegian University of Science and Technology (NTNU)
Trondheim, Norway
oystein.sture at ntnu.no

Terje Thorsnes
Department of Marine Geology
Geological Survey of Norway (NGU)
Trondheim, Norway

***Abstract*—The deep-water coral *Lophelia pertusa* is a common reef-building scleractinian coral, or stony coral, occurring in mid to deep waters around the world. The reefs they form are regarded as hot spots for biodiversity and carbon cycling, and play a key role in benthic ecosystems in Norwegian waters. The cold-water reefs are however under increasing anthropogenic pressure due to human activities and a changing environment. Development of methods that enable time- and cost-effective monitoring of these reefs is therefore important. We propose using synthetic aperture sonar (SAS) on-board autonomous underwater vehicles (AUVs) as a means to detect the presence of assemblages of corals. Automated segmentation of areas with coral is presented using a convolutional neural network (CNN).**

***Index Terms*—Lophelia pertusa, AUV, Synthetic Aperture Sonar, Convolutional Neural Network**

I. Introduction

Lophelia pertusa [1] grows globally on continental slopes, oceanic ridges, and in fjords. Its geographical distribution extends throughout the North Atlantic, including parts of the Mediterranean, as well as down both sides of the Atlantic along the coasts of West Africa and Americas, and in scattered locations around the world. In the North Atlantic, they are generally found in depths of $200\,\mathrm{m}$ to $1000\,\mathrm{m}$, with the exception of some Norwegian and Swedish fjords. In mid-Norway (62°30'-65°30'N), individual reefs can extend across $1230\,\mathrm{m}^2$ to $37.310\,\mathrm{m}^2$ with the total coverage estimated at approximately $35\,\mathrm{km}^2$ [2]. The bioherms they form has been observed to cover up to a vertical height of $31\,\mathrm{m}$ [3].

The coral reef structures provide a three-dimensional environment, which serves as a shelter for other species, facilitates sediment deposition and promotes abundance and diversity of fauna. The reefs have been linked to macrofaunal communities distinct from non-coral soft-sediment environments [4]. Data also indicate that these reefs have a very important functional role in deep-water ecosystems as fish habitats, and perhaps as breeding grounds and/or nursery habitats [5]. Other corals, such as *Madrepora oculata*, often occur together with *Lophelia*, but have not been reported to form coral reefs by themselves [2]. *Lophelia* reefs are regarded as hot spots for biodiversity and carbon cycling, and play a key role in benthic ecosystems in Norwegian waters.

Figure 1 shows a map of the confirmed locations of *Lophelia* in Norwegian waters and protected zones in which bottom trawling is prohibited. It can be seen that the reefs have a tendency to grow either on areas of steep bathymetry or in fjords, where the current supplies sufficient food. The Norwegian shelf is host to around $30\,\%$ of the known occurrences in the world [9].

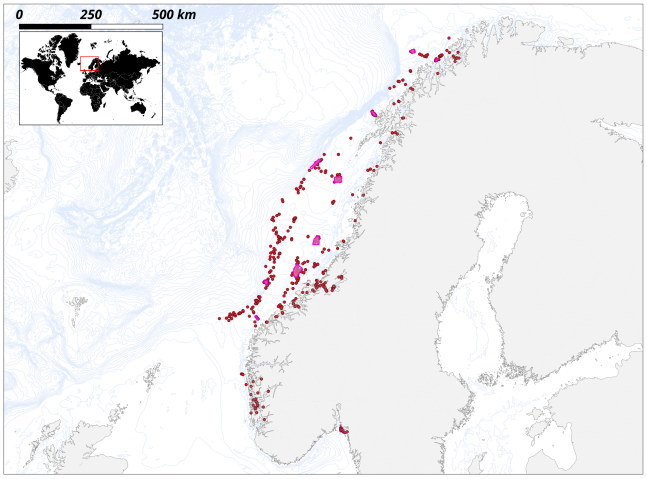

Fig. 1. Locations of known sites with *Lophelia pertusa* growth in Norwegian waters (red markers). Purple polygons are protected areas in which trawling is not permitted [6]–[8].

The cold-water reefs are however under increasing anthropogenic pressure due to human activities and a changing environment, in particular bottom trawling and acidification of the oceans [9], [10]. The *Lophelia* corallites themselves grow $5\,\mathrm{mm}$ to $10\,\mathrm{mm}$ per year and the growth rate of a *Lophelia* reef is estimated to be $1.3\,\mathrm{mm\,yr}^{-1}$ [11], [12]. For this reason, the recovery time in terms of biological function is significant [13]. In the absence of coral production, the coral structures are dissolved through physical, chemical and biological processes [14]. The rate at which this occurs may increase due to ocean acidification (OA) and exceed the growth rate of warm-water coral reefs [15]. *Lophelia* has been shown to better acclimate to elevated CO_2 exposure in the long-term [16], but may come at the cost of reduced respiratory rates — implying the use of stored energy to maintain calcification rates [17]. The exposed coral framework, i.e. not covered by protective tissue,

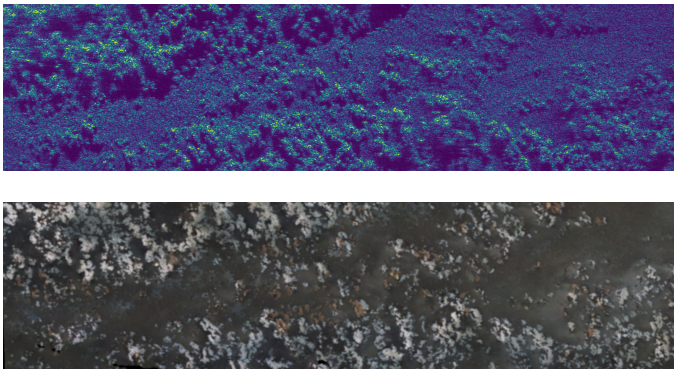

Fig. 2. Synthetic aperture sonar and orthomosaic of ROV video footage taken from the same area. The corals can be identified from their morphology. The colormap ranges from blue to yellow (viridis), where the latter indicates a strong acoustic response. The spatial extent is $16.3 \times 38.4\,\mathrm{m}$

becomes structurally weaker in high CO_2 conditions, possibly impacting the structural integrity of the reefs despite the acclimation of the live corals [18]. The presence of multiple stressors, such as a combination of elevated temperature and CO_2, have recently been shown to impair growth rates during times of increased food availability despite a positive response when only one is present [19]. The aforementioned issues highlights the need for long-term monitoring, and establishing a baseline is something that should be done sooner rather than later.

We define a coral reef as a local seafloor mound consisting of accumulations of coral debris, fine-grained and sometimes course-grained sediments, and live coral colonies [20]. The intact *Lophelia* structures can be recognized from their distinct cauliflower-patterned texture. This pattern has previously been observed in SAS imagery, and confirmed to be corals through video and hyperspectral imagery from a remotely operated vehicle (ROV) [21]. In this work, we are concerned with detection of the microhabitats that impact the sonar imagery due to their morphology. Namely, the separation of living and dead intact coral structures from sediments, rubble and other facies. The separation of recently dead coral with intact structures from living corals is discussed, but not addressed through this work. Local extinction events, such as from bottom trawling, should be able to be detected due to the physical impact on the morphology — provided that the same area is visited both before and after the event.

Coral reefs have been studied in acoustic data for a long time, and have been found to have an imprint on multibeam backscatter data and multi-frequency echosounders [22], [23]. It is worth mentioning that corals will need a hard substrate on which to grow - which may also affect the backscattering strength relative to the surrounding sediments. Regular side-scan sonar has also been used to detect reefs, where the approaches are often based on aggregated statistics such as seabed scattering roughness due to the limited spatial resolution [24], [25].

More recently, several bathymetric derivatives, such as curvature and roughness, have been shown to be able to predict the location of deep-water coral mounds by utilizing a random forest classification [26], [27]. This method can predict regions where the presence of coral reefs is probable, but does not directly detect presence of corals themselves or differentiate between living and dead corals. The approach is useful for coastal and oceanic management and narrowing down the areas of interest for further studies.

The remainder of the paper is organized as follows. We first briefly cover the technologies used; synthetic aperture sonar and convolutional neural networks. The data sets are then introduced and pre-processing is described. The classification results are then presented and discussed in the context of coastal management and autonomous underwater vehicles.

II. Methods

A. Synthetic Aperture Sonar

Given the vast and scattered areas covered by these coral reefs, sonar technology is ideal for obtaining high coverage rates for abundance mapping. Synthetic aperture sonar (SAS) differs from regular side-scan sonars by utilizing multiple pings to reconstruct a single spatial location in the output image during post-processing. The main benefits over regular side-scan sonar are improvements in the along-track resolution and a range-independent resolution. The signal-to-noise ratio is still range-dependent however, which causes a reduction in image quality with range. SAS processing imposes additional constraints on navigational accuracy however, as the position and orientation of the sensor must be accurately estimated for each part of the synthetic array [28]. An autonomous underwater vehicle (AUV) is especially suited as a platform for SAS, as its movement is slow and stable, and generally has high quality inertial navigational sensors. The inclusion of SAS on an AUV can also be beneficial for the performance of the overall system. The ping-to-ping displacement (micro-navigation) is estimated during SAS processing and can be integrated with the inertial navigation system (INS) to improve the overall navigational accuracy [29]. If the SAS has an interferometric capability, terrain-navigation can also be applied to overlapping swaths (macro-navigation) [30]. This matches well up with the current trend of making AUVs more autonomous. Using the parent ship for other tasks, such as target checking corals with an ROV, while the AUV is performing its mission is achievable.

SAS images are well suited for the purpose of classification, not only due to their higher overall resolution, but especially due to the range-independent resolution. Classification with filters operating in the spatial domain can be developed based around the assumption that the spatial frequencies will be homogeneous throughout the swath for the same object; except for the presence of speckle.

B. Convolutional Neural Networks

Convolutional neural networks (CNN) are neural networks in which the convolution operator is utilized at some point between spatial and/or temporal data and a convolution kernel.

The hyper-parameters of the kernel are typically included in the training process (e.g. updated through back-propagation). It has seen much use in image and audio processing in recent years, as spatial and temporal features can be learned from the data itself and the convolution operation is efficient on modern hardware. The alternative to learning the spatial or temporal filters from the data is manual or externally optimized feature selection through statistical operators, designed filter kernels or similar approaches. The design of a neural network has its challenges however, especially if the data set is small in relation to the number of free hyperparameters. Parameters such as learning rate and momentum must carefully be tweaked depending on the data set and network to avoid getting stuck in local optima.

We propose the use of convolutional neural networks (CNN) to classify the presence of deep-water corals in synthetic aperture sonar (SAS) imagery as a tool for doing large-scale monitoring. The convolutional filter-banks are trained to detect these textures, and the CNN is able to separate them from sand or rock facies that does not exhibit similar textures. CNNs are well suited for the task, as they are invariant to translation and is able to learn filters at multiple scales to account for differently sized corals.

C. Data Acquisition

This work is based on data collected during fieldwork in 2012, 2013 and 2017. The main area is the Tautra Ridge in the Trondheimsfjord, where an area of approximately $2.7\,\mathrm{km}^2$ has been covered. Another reef at Nord-Leksa, also in the Trondheimsfjord, was covered with an area of $2.9\,\mathrm{km}^2$. These reefs are among the most shallow cold-water coral reefs in the world, with Tautra largely situated between $30\,\mathrm{m}$ to $60\,\mathrm{m}$ depth. The locations of these reefs are presented in figure 3. The Nord-Leksa reef was kept as a verification data set, and not used during training. This avoids skewing the classification accuracy due to the possibility that the training and verification was performed on the same corals, as there is significant overlap across the different years on Tautra.

The data set was collected with the autonomous underwater vehicle (AUV) Hugin HUS 1000 from Kongsberg Maritime, and a Kongsberg HiSAS 1030 synthetic aperture sonar system, operated by the Norwegian Defense Research Establishment (FFI). During the collection, an average altitude of $26\,\mathrm{m}$ above the seabed was maintained, with a slant range of around $150\,\mathrm{m}$.

D. Preprocessing and classes

Post-processing was performed using the Kongsberg FOCUS toolbox and subsequently gridded to $4\,\mathrm{cm} \times 4\,\mathrm{cm}$ mosaics with Kongsberg Reflection, joining the survey lines and ensuring a constant spatial resolution. The mosaics were split into sub-images of 100x100 pixels, and hand-labeled to two classes; one with corals and one with other seabed features — such as sediments, rocks, and shadows. The data set contained 16 358 images of corals. The labeling was performed based on a map delineated from video transects collected with a remotely operated vehicle (ROV). We acknowledge that the ground truth labeling is based on a subjective interpretation in the cases where an ROV transect does not overlap exactly, which may introduce a bias in the perceived accuracy.

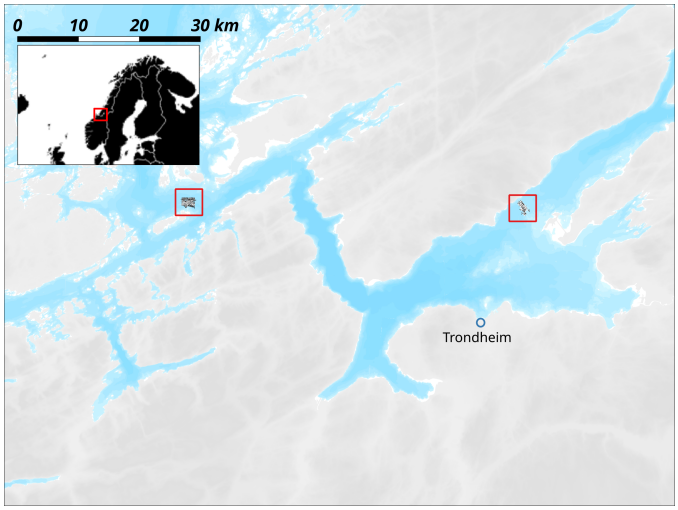

Fig. 3. The locations of the collected data sets. Marked area to the west is the Nord-Leksa reef, while the easternmost is the Tautra reef [7].

E. Network Structure

The network structure is composed of four blocks of convolution. Each block contains a convolutional layer (5x5) followed by a batch normalization layer [31], rectified linear (ReLu) activation function [32] and a max-pooling operation [33]. These operations are repeated for each of the blocks, with the number of filters in the convolution kernels doubling for each following block. The output from the last block is flattened and passed through two dense (fully connected) layers with a dropout function in between [34]. The final dense layer has a softmax activation to normalize the output, such that it can be interpreted as a measure of probability. The dropout and batch normalization layers are there to prevent overfitting and improve the training rates of the network.

TABLE I
NEURAL NETWORK ARCHITECTURE

Layer	Output size
Input image	100x100x1
Convolution block 1	48x48x32
Convolution block 2	22x22x64
Convolution block 3	9x9x128
Convolution block 4	2x2x256
Flatten	1024
Dense (ReLu)	507
Dropout (0.25)	507
Dense (Softmax)	2

The weights and biases of the convolutional kernels and dense layers are trained by an optimizer. The optimizer is what essentially takes the loss function in the final layer and updates the hyperparameters incrementally. We utilize the Adam algorithm, which computes individual adaptive learning rates based on the first and second moments of the gradient of

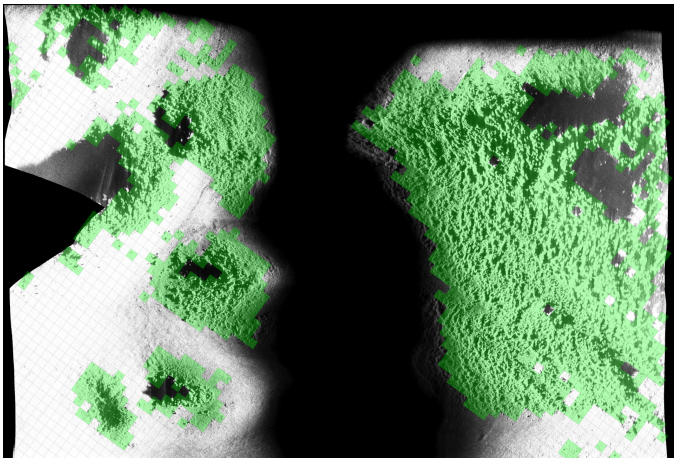

Fig. 4. Classification of corals on Tautra validation set from 2017. Green areas are classified as patches with coral presence. The spatial extent is $300 \times 200\,\mathrm{m}$

the loss function [35]. There are additional hyperparameters not trained by the optimizer however; such as the parameters for the optimizer itself, number of filters in the convolution layers, and dropout rates. These were determined through a grid-search approach [36], where the network was evaluated against the test data set for different combinations of parameter values.

The network was implemented both in the MATLAB Deep Learning Toolbox™and Keras with Tensorflow as the backend [37], [38]. The final results were produced in the latter. The network was trained on a computer with Intel® Core™ i7-7020X CPU and a Nvidia GeForce GTX 1080 Ti GPU.

III. Results

The images were divided into 20% validation data, 20% testing data and the remainder for training. The testing data were used to tune the hyperparameters, and the validation data were used to determine the final accuracy of the classifier, without biasing the result.

The final classifier was tested on verification images, which were not directly included in the training process. It should however be noted that the same regions from Tautra might be in the training set due to overlapping transects in different years. The Nord-Leksa data set is however completely separate, as it is from a reef not used in the training process. The results can be seen in table II. We use the true positive rate (TPR) and true negative rate (TNR), sometimes called recall and specificity, to denote the classification rates. These are defined by

$$\text{TPR} = \frac{TP}{TP + FN} \quad \text{and} \quad \text{TNR} = \frac{TN}{TN + FP}$$

where TP/TN denotes the true positive and true negative classified images, and FP/FN denotes the false positives and false negatives respectively.

The 2012 verification data set has more sparsely populated and scattered corals than the other data sets, and has the lowest detection rate of corals a result. The classifier is based around recognition of assemblages of corals, and is struggling with image subsets with solitary corals. The verification data set from the Nord-Leksa reef has a reduction in the attainable rates compared to the Tautra data sets, but is still within acceptable classification accuracy.

TABLE II
Verification data set results

data set	TPR	TNR
Tautra 2012	80.4%	95.9%
Tautra 2013	92.6%	96.0%
Tautra 2017	94.9%	97.2%
Nord-Leksa 2013	88.7%	91.7%

IV. Discussion

We see that the classification results are overall quite high, with a tendency to classify corals as the other class rather than erroneously classifying other seabed features as corals. The likely reason for this is that the number of images from each class is imbalanced. The penalty (loss) for misclassifying images during training must be calculated with an appropriate weight to account for the relative size difference of the data set. While this is generally straightforward, the class containing non-coral images is composed of multiple phenomena, such as instances of shadows, sediments, oversaturated areas, distorted/non-intelligible images, and edges of the mosaic (background). The class is therefore imbalanced within itself, and applying a weight to account for the difference in samples between the two classes would not solve the problem. To truly make up for the unbalanced number of samples, the penalty for classifying the other class wrongly would therefore need to be different on a per-sample basis - thus reflecting the number of samples representing e.g. shadows or sediments accurately within the class. This was not done for the classifier trained here, and is left to future work.

In certain areas the labelling has been performed contextually with respect to the spatial locality. Areas sparsely populated with corals at the edges of the reef or in an area consisting of predominately dense coral mounds were also labeled as corals. The classifier does not consider the neighbourhood outside the size of the input image. If the classifier has problems misclassifying other seabed features such as rocks as corals, removing these images of sparsely populated corals could make the classifier more robust. The Nord-Leksa reef is also distributed more sparsely than Tautra. Including most of the Nord-Leksa data set into the training process except for a spatial subset reserved for verification, rather than excluding the entire reef in the training, would likely attain better classification rates on sparsely populated corals. Collection of more data is however needed to better assess the performance when applied to more variable seabed features.

An interesting topic that has not been investigated in this work, is the directional component of the coral mounds. The corals grows in such a way that the surface area is large

towards the source of nutrients. It is plausible to believe that the sonar images should reflect this, with features that are more thin and elongated when seen from the side. Investigation of this may require the AUV to map across the bathymetric contours rather than along them however — impacting both data quality and operational safety of the vehicle.

A. Coral State Detection

An important question that so far hasn't been answered, is the applicability of this method and sonar imagery to determine the state of corals in the instance where they are dead or dying, but still intact in shape. Only approximately the outermost meter of corallites contains live polyps, while older polyps beneath die due to reduced water exchange and food supply [39], [40]. We can thus divide a reef into three habitats; coral rubble zone with small pieces of skeleton, followed by the coral block zone dominated by large blocks of coral skeleton, and finally the live coral reef on top where the current provides food [41]. This transition between the zones may impact the shape or regularity of the mound structures in the sonar imagery. More studies with basis in video footage is needed to determine how accurately these changes can be observed in sonar imagery. The speed at which the coral block zone is converted to rubble may also increase as a result of ocean acidification. The application of change-detection in SAS imagery has previously been proposed to detect changing trends in coral coverage, but does require high positional accuracy across the data sets [42]. The use of change detection on corals has previously been demonstrated, but can be challenging in areas of rough topography and/or variable ocean environments [43]. Regardless of the applicability of SAS to detection of coral death induced by environmental factors, change detection can be useful for detection of local extinction events (e.g. from bottom trawling).

Both living and dead corals has been observed to be covered in a crust of Fe/Mg, but live corals are less afflicted due to protective soft tissue [44]. This could possibly change the acoustic reflectivity of the corals, but might be frequency dependent or not feasible to detect at all using conventional sonar technology.

B. In-Situ Classification

The work described here was performed offline. Moving the classification on-board the AUV itself can facilitate recognition of corals during the mission. Synthetic aperture sonar can be processed in real-time inside an AUV, provided that it is is equipped with enough processing capability, at the expense of additional weight, volume, and power consumption [45]. This has for example been used in automatic target recognition of mine-like objects, and other online-adaptations to improve the data quality [46]. In terms of coral surveying, this could enable automated near-seabed camera coverage of coral patches to be able to better assess the coral state and perform automated abundance estimation [47]. Larger reefs have a tendency to grow elongated, facing towards the main current [41]. Efficiency in mapping large, elongated reefs could be improved by determining where to survey based on the observed coral densities in-situ, to avoid spending time unnecessarily imaging surrounding sediments.

With these goals in mind, the performance of the network during inference was evaluated on a Nvidia Jetson TX2 embedded system, operating in its highest performance mode (Max-N). The maximum thermal design power envelope for the board is $15\,\mathrm{W}$. The pre-trained network was evaluated on a batch of 100 images repeated 1000 times, which took $197.4\,\mathrm{s}$. This results in a processing capability of $100000/197.4\,\mathrm{s} = 506.6$ images per second. With an image envelope of $4\,\mathrm{m}^2$, as used in this work, this results in an area processing rate of $4\,\mathrm{m}^2 \cdot 506.6 = 2026.4\,\mathrm{m}^2/\mathrm{s}$. Given an AUV speed of $2.0\,\mathrm{m\,s}^{-1}$ and a ground range of $150\,\mathrm{m}$, the area coverage rate of the sonar is $2.0\,\mathrm{m\,s}^{-1} \cdot 150\,\mathrm{m} \cdot 2 = 600\,\mathrm{m}^2/\mathrm{s}$ for both sides. We see that online processing is feasible, and leaves much headroom to optimize the performance in terms of energy usage, target resolution or network size.

V. Conclusion

A convolutional neural network capable of classifying the presence of *Lophelia pertusa* in synthetic aperture sonar images has been presented. The network has been shown to attain high classification rates on the verification data, and have been shown to be light enough computationally for online processing, provided that real-time synthetic aperture sonar processing is available. While there are still questions to be answered with respect to the classification performance in the presence of greater variability in seabed features, we feel that this is an important step towards better methodology for coastal management with respect to cold-water corals on a medium- to large-scale. Determining whether coral state estimation based on morphology, change-detection, or acoustic backscatter, are natural extensions to this work.

Acknowledgment

This work is based on data gathered with Kongsberg Hugin HUS 1000, operated by the Norwegian Defence Research Establishment (FFI). The work is based on the master thesis of Margrete S. Scheide [48]. The maps are based on the following open data sources [6]–[8], and produced in Quantum GIS [49]. The orthomosaic in figure 2 was made by Stein M. Nornes.

References

[1] C. v. Linnaeus, "Systema naturae per regna tria naturae. secundum classes, ordines, genera, species, cum characteribus, differentiis, synonymis, locis," *Editio*, vol. 1, no. 10, p. 823, 1758.

[2] P. B. Mortensen, T. Hovland, J. H. Fosså, and D. M. Furevik, "Distribution, abundance and size of *Lophelia pertusa* coral reefs in mid-Norway in relation to seabed characteristics," *Journal of the Marine Biological Association of the United Kingdom*, vol. 81, no. 4, pp. 581–597, 2001.

[3] P. B. Mortensen, M. Hovland, T. Brattegard, and R. Farestveit, "Deep water bioherms of the scleractinian coral *Lophelia pertusa* (L.) at 64 N on the Norwegian shelf: structure and associated megafauna," *Sarsia*, vol. 80, no. 2, pp. 145–158, 1995.

[4] A. W. Demopoulos, J. R. Bourque, and J. Frometa, "Biodiversity and community composition of sediment macrofauna associated with deep-sea *Lophelia pertusa* habitats in the Gulf of Mexico," *Deep Sea Research Part I: Oceanographic Research Papers*, vol. 93, pp. 91–103, 2014.

[5] M. J. Costello, M. McCrea, A. Freiwald, T. Lundälv, L. Jonsson, B. J. Bett, T. C. van Weering, H. de Haas, J. M. Roberts, and D. Allen, "Role of cold-water *Lophelia pertusa* coral reefs as fish habitat in the NE Atlantic," in *Cold-water corals and ecosystems*. Springer, 2005, pp. 771–805.

[6] P. B. Mortensen, "*Lophelia pertusa* reefs in Norwegian seawaters," Norwegian Marine Data Centre (nmdc.no), 09 2018.

[7] Norwegian Mapping Authority (Kartverket), "Europe Basemap WMS," geonorge.no, ©Kartverket.

[8] MAREANO/Institute of Marine Research, "Marine protected areas WMS," imr.no.

[9] J. Järnegren and T. Kutti, "*Lophelia pertusa* in Norwegian waters. What have we learned since 2008?" Norwegian Institute for Water Research, Tech. Rep., 2014.

[10] J. M. Roberts, A. J. Wheeler, and A. Freiwald, "Reefs of the deep: the biology and geology of cold-water coral ecosystems," *Science*, vol. 312, no. 5773, pp. 543–547, 2006.

[11] P. B. Mortensen, H. T. Rapp, and U. Båmstedt, "Oxygen and carbon isotope ratios related to growth line patterns in skeletons of *Lophelia pertusa* (L)(Anthozoa, Scleractinia): Implications for determination of linear extension rate," *Sarsia*, vol. 83, no. 5, pp. 433–446, 1998.

[12] P. B. Mortensen, "*Lophelia pertusa* (Scleractinia) in Norwegian waters. distribution, growth, and associated fauna." Ph.D. dissertation, University of Bergen (UiB), 2000.

[13] J. H. Fosså, P. Mortensen, and D. M. Furevik, "The deep-water coral *Lophelia pertusa* in Norwegian waters: distribution and fishery impacts," *Hydrobiologia*, vol. 471, no. 1-3, pp. 1–12, 2002.

[14] B. D. Eyre, A. J. Andersson, and T. Cyronak, "Benthic coral reef calcium carbonate dissolution in an acidifying ocean," *Nature Climate Change*, vol. 4, no. 11, p. 969, 2014.

[15] B. D. Eyre, T. Cyronak, P. Drupp, E. H. De Carlo, J. P. Sachs, and A. J. Andersson, "Coral reefs will transition to net dissolving before end of century," *Science*, vol. 359, no. 6378, pp. 908–911, 2018.

[16] A. U. Form and U. Riebesell, "Acclimation to ocean acidification during long-term co2 exposure in the cold-water coral lophelia pertusa," *Global Change Biology*, vol. 18, no. 3, pp. 843–853, 2012.

[17] S. Hennige, L. Wicks, N. Kamenos, D. C. Bakker, H. Findlay, C. Dumousseaud, and J. Roberts, "Short-term metabolic and growth responses of the cold-water coral lophelia pertusa to ocean acidification," *Deep Sea Research Part II: Topical Studies in Oceanography*, vol. 99, pp. 27–35, 2014.

[18] S. Hennige, L. Wicks, N. Kamenos, G. Perna, H. Findlay, and J. Roberts, "Hidden impacts of ocean acidification to live and dead coral framework," *Proc. R. Soc. B*, vol. 282, no. 1813, p. 20150990, 2015.

[19] J. V. Büscher, A. U. Form, and U. Riebesell, "Interactive effects of ocean acidification and warming on growth, fitness and survival of the cold-water coral lophelia pertusa under different food availabilities," *Frontiers in Marine Science*, vol. 4, p. 101, 2017.

[20] M. Hovland, *Deep-water coral reefs: Unique biodiversity hot-spots*. Springer Science & Business Media, 2008.

[21] M. Ludvigsen, G. Johnsen, A. J. Sørensen, P. A. Lågstad, and Ø. Ødegård, "Scientific operations combining ROV and AUV in the Trondheim Fjord," *Marine Technology Society Journal*, vol. 48, no. 2, pp. 59–71, 2014.

[22] J. Roberts, C. Brown, D. Long, and C. Bates, "Acoustic mapping using a multibeam echosounder reveals cold-water coral reefs and surrounding habitats," *Coral Reefs*, vol. 24, no. 4, pp. 654–669, 2005.

[23] J. H. Fosså, B. Lindberg, O. Christensen, T. Lundälv, I. Svellingen, P. B. Mortensen, and J. Alvsvåg, "Mapping of *Lophelia pertusa* reefs in Norway: experiences and survey methods," in *Cold-water corals and ecosystems*. Springer, 2005, pp. 359–391.

[24] B. Lindberg, C. Berndt, and J. Mienert, "The Fugløy Reef at 70 N; acoustic signature, geologic, geomorphologic and oceanographic setting," *International Journal of Earth Sciences*, vol. 96, no. 1, pp. 201–213, 2007.

[25] V. Huvenne, P. Blondel, and J.-P. Henriet, "Textural analyses of sidescan sonar imagery from two mound provinces in the Porcupine Seabight," *Marine Geology*, vol. 189, no. 3-4, pp. 323–341, 2002.

[26] L. De Clippele, J. Gafeira, K. Robert, S. Hennige, M. Lavaleye, G. Duineveld, V. Huvenne, and J. Roberts, "Using novel acoustic and visual mapping tools to predict the small-scale spatial distribution of live biogenic reef framework in cold-water coral habitats," *Coral Reefs*, vol. 36, no. 1, pp. 255–268, 2017.

[27] M. Diesing and T. Thorsnes, "Mapping of cold-water coral carbonate mounds based on geomorphometric features: An object-based approach," *Geosciences*, vol. 8, no. 2, p. 34, 2018.

[28] R. E. Hansen, "Synthetic aperture sonar technology review," *Marine Technology Society Journal*, vol. 47, no. 5, pp. 117–127, 2013.

[29] R. E. Hansen, T. O. Saebo, K. Gade, and S. Chapman, "Signal processing for auv based interferometric synthetic aperture sonar," in *OCEANS 2003. Proceedings*, vol. 5. IEEE, 2003, pp. 2438–2444.

[30] P. E. Hagen, O. Midtgaard, and O. Hasvold, "Making auvs truly autonomous," in *OCEANS 2007*. IEEE, 2007, pp. 1–4.

[31] S. Ioffe and C. Szegedy, "Batch normalization: Accelerating deep network training by reducing internal covariate shift," *arXiv preprint arXiv:1502.03167*, 2015.

[32] V. Nair and G. E. Hinton, "Rectified linear units improve restricted boltzmann machines," in *Proceedings of the 27th international conference on machine learning (ICML-10)*, 2010, pp. 807–814.

[33] D. Scherer, A. Müller, and S. Behnke, "Evaluation of pooling operations in convolutional architectures for object recognition," in *Artificial Neural Networks–ICANN 2010*. Springer, 2010, pp. 92–101.

[34] N. Srivastava, G. Hinton, A. Krizhevsky, I. Sutskever, and R. Salakhutdinov, "Dropout: a simple way to prevent neural networks from overfitting," *The Journal of Machine Learning Research*, vol. 15, no. 1, pp. 1929–1958, 2014.

[35] D. P. Kingma and J. Ba, "Adam: A method for stochastic optimization," *arXiv preprint arXiv:1412.6980*, 2014.

[36] I. Goodfellow, Y. Bengio, and A. Courville, *Deep Learning*. MIT Press, 2016.

[37] F. Chollet *et al.*, "Keras," https://keras.io, 2015.

[38] M. Abadi, A. Agarwal, P. Barham, E. Brevdo, Z. Chen, C. Citro, G. S. Corrado, A. Davis, J. Dean, M. Devin, S. Ghemawat, I. Goodfellow, A. Harp, G. Irving, M. Isard, Y. Jia, R. Jozefowicz, L. Kaiser, M. Kudlur, J. Levenberg, D. Mané, R. Monga, S. Moore, D. Murray, C. Olah, M. Schuster, J. Shlens, B. Steiner, I. Sutskever, K. Talwar, P. Tucker, V. Vanhoucke, V. Vasudevan, F. Viégas, O. Vinyals, P. Warden, M. Wattenberg, M. Wicke, Y. Yu, and X. Zheng, "TensorFlow: Large-scale machine learning on heterogeneous systems," 2015, software available from tensorflow.org. [Online]. Available: https://www.tensorflow.org/

[39] J. Wilson, "Patch development of the deep-water coral *Lophelia pertusa* (L.) on Rockall Bank," *Journal of the Marine Biological Association of the United Kingdom*, vol. 59, no. 1, pp. 165–177, 1979.

[40] S. M. Strömberg and C. Östman, "The cnidome and internal morphology of *Lophelia pertusa* (Linnaeus, 1758)(Cnidaria, Anthozoa)," *Acta Zoologica*, vol. 98, no. 2, pp. 191–213, 2017.

[41] L. Buhl-Mortensen, A. Vanreusel, A. J. Gooday, L. A. Levin, I. G. Priede, P. Buhl-Mortensen, H. Gheerardyn, N. J. King, and M. Raes, "Biological structures as a source of habitat heterogeneity and biodiversity on the deep ocean margins," *Marine Ecology*, vol. 31, no. 1, pp. 21–50, 2010.

[42] M. Ludvigsen, T. Thorsnes, R. E. Hansen, A. J. Sørensen, G. Johnsen, P. A. Lågstad, Ø. Ødegård, M. Candeloro, S. M. Nornes, and C. Malmquist, "Underwater vehicles for environmental management in coastal areas," in *OCEANS 2015-Genova*. IEEE, 2015, pp. 1–6.

[43] R. Hansen, T. Sæbø, O. Lorentzen, and Ø. Midtgaard, "Change detection in topographic structures using interferometric synthetic aperture sonar," in *Proceedings of the 2st Underwater Acoustic Conference*, 2014.

[44] A. Freiwald, R. Henrich, and J. Pätzold, "Anatomy of a deep-water coral reef mound from Stjernsund, West Finnmark, northern Norway," 1997.

[45] "HISAS: High resolution Interferometric Synthetic Aperture Sonar (brochure)," 2018, hisas_1030_brochure_v1_lowres_v2.pdf.

[46] F. Baralli, M. Couillard, J. Ortiz, and D. G. Caldwell, "GPU-based real-time synthetic aperture sonar processing on-board autonomous underwater vehicles," in *OCEANS-Bergen, 2013 MTS/IEEE*. IEEE, 2013, pp. 1–8.

[47] A. Purser, M. Bergmann, T. Lundälv, J. Ontrup, and T. W. Nattkemper, "Use of machine-learning algorithms for the automated detection of cold-water coral habitats: a pilot study," *Marine Ecology Progress Series*, vol. 397, pp. 241–251, 2009.

[48] M. S. Scheide, "Using Deep Learning for Automatic Classification of Marine Habitats in HiSAS Imagery." Master's thesis, NTNU, 2018.

[49] QGIS Development Team, "Quantum gis geographic information system. open source geospatial foundation project," 2018.